INSTITUTE OF PHYSICS PUBLISHING JOURNAL OF PHYSICS B: ATOMIC, MOLECULAR AND OPTICAL PHYSICS

J. Phys. B: At. Mol. Opt. Phys. **36** (2003) 1–9 PII: S0953-4075(03)38239-2

The ejection of a correlated electron pair from a quantum dot

N Fominykh, O Kidun, A Ernst and J Berakdar

Max-Planck Institut für Mikrostrukturphysik, Weinberg 2, 06120 Halle, Germany

E-mail: fom@mpi-halle.de

Received 12 June 2002, in final form 15 November 2002
Published 20 December 2002
Online at stacks.iop.org/JPhysB/36/1

Abstract

We use the exact initial two-electron states of the parabolic potential well to calculate the double photoemission (DPE) spectra of a quantum dot. Being exactly solvable, the problem of two electrons coupled by a Coulomb interaction in an oscillator confinement provides a unique test for any approximate theories that deal with few-body systems and related experiments. An instructive treatment based on a direct mapping of a two-electron initial state density onto the DPE observables is proposed, which clearly explains how the DPE spectra are organized and gives some hints for their experimental measurement.

(Some figures in this article are in colour only in the electronic version)

1. Introduction

The evaluation of the effects of electronic correlations must be included in most of the theories dealing with electronic excitations by external fields. While for some processes (e.g. single photoemission [1, 2]) inclusion of the correlations involved leads only to the refinement of the calculated transition probabilities (which otherwise can be calculated in the independent-electron approximation), for some other processes (e.g. [3, 4]) they are a vital ingredient of the theoretical description, playing a major role in determining the characteristics of the process. In the latter case the careful use of approximations is important, for it is possible that the features introduced by some aggressive approximations may become even more pronounced than those that are inherent to a very physical process. Therefore, it is important to have a reference among the exactly solvable models to be able to judge the quality of the approximate solutions.

One such process, which occurs as a result of the electron–electron interaction and is impossible in the independent-electron case [4], is double photoemission (DPE). In DPE the absorption of a photon by a system results in the simultaneous emission of a pair of electrons. In a schematic way it can be described by a diagram such as figure 1, where the bold line represents the exact two-electron initial and final states Φ_2 and Ψ_2, respectively, and the wavy line depicts

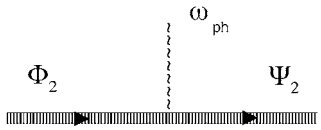

Figure 1. Diagrammatic representation of DPE: the two-particle state Φ_2 evolves into the two-particle state Ψ_2 by absorbing a photon with energy ω_{ph}.

a photon with energy ω_{ph}. In general, the problem of two interacting electrons in the external potential does not have an exact solution. However, for a particular case of a parabolic potential well the two-electron eigenstates can be found without approximations [6], and we believe it is of methodological importance to consider the one-photon ionization of such a system. Physical systems that exhibit an electronic structure and are well reproduced by oscillator confinement are semiconductor quantum dots [7]. In the present paper we consider the DPE from a single quantum dot. We start from the brief overview of the exact solution (section 2), write down the expressions for the differential cross section of the process (section 3) and calculate the DPE angular (section 4) and energy (section 5) distributions for the typical parameters of a quantum dot. The mapping of the initial-state density onto the DPE spectra, discussed in sections 4 and 5, aims to illustrate the DPE distributions and to facilitate a choice of the observation conditions for future experiments.

2. Exact solution

More details on the problem can be found in the recent paper by Taut *et al* [6]; here we only give the expressions that are needed for our purposes. For the description of a semiconductor medium we assume the effective mass approximation (m^* is taken in units of the bare electron mass) and the weakening of the Coulomb interaction by the static dielectric constant ϵ. Atomic units are used throughout.

Upon the transformation to the centre-of-mass (CM) and relative coordinates

$$\boldsymbol{R} = \tfrac{1}{2}(\boldsymbol{r}_1 + \boldsymbol{r}_2), \qquad \boldsymbol{r} = \boldsymbol{r}_1 - \boldsymbol{r}_2, \tag{1}$$

the Hamiltonian for two interacting electrons in the parabolic well

$$H = -\frac{1}{2m^*}\nabla_{r_1}^2 - \frac{1}{2m^*}\nabla_{r_2}^2 + \frac{1}{2}m^*\omega^2 {r_1}^2 + \frac{1}{2}m^*\omega^2 {r_2}^2 + \frac{1}{\epsilon|\boldsymbol{r}_1 - \boldsymbol{r}_2|} \tag{2}$$

can be expressed as a sum of two independent parts

$$H = -\frac{1}{4m^*}\nabla_R^2 - \frac{1}{m^*}\nabla_r^2 + \frac{m^*}{4}\omega^2 r^2 + m^*\omega^2 R^2 + \frac{1}{\epsilon r} \equiv H_R + H_r, \tag{3}$$

with the two-electron wavefunction also being separable in these coordinates

$$\Phi_2(1,2) = \varphi(\boldsymbol{r}) \cdot \xi(\boldsymbol{R}) \cdot \chi(s_1, s_2). \tag{4}$$

The total energy is then given by the sum of the eigenenergies E_R and E_r of H_R and H_r, respectively

$$E = E_R + E_r. \tag{5}$$

As is usual for the spin-independent Hamiltonians, the Pauli principle is guaranteed in that the spin part of the wavefunction $\chi(s_1, s_2)$ has to be chosen to be symmetric or antisymmetric (with respect to particle exchange) in accordance with the symmetry of its coordinate part.

The Schrödinger equation for the CM motion coincides with the equation for the three-dimensional harmonic oscillator

$$\left[-\frac{1}{2m^*}\nabla_{\boldsymbol{R}}^2+\frac{1}{2}m^*\omega_R^2R^2\right]\xi(\boldsymbol{R})=E'_R\xi(\boldsymbol{R}),\qquad \omega_R\equiv 2\omega,\ E'_R\equiv 2E_R, \quad (6)$$

and has analytical solutions [8], that are classifiable according to the node number N and orbital momentum quantum number L

$$\xi_{NLM}(\boldsymbol{R})=\frac{U_{NL}(R)}{\sqrt{m^*}R}Y_{LM}(\hat{\boldsymbol{R}}),\qquad N=0,1,2\ldots,\ L=0,1,2\ldots, \quad (7)$$

where the radial function is given in terms of the confluent hypergeometric functions [9]

$$U_{NL}(R)=(\sqrt{m^*}R)^{L+1}\exp\left(-\frac{m^*\omega}{2}R^2\right)F\left(-N,\,L+\frac{3}{2};\,m^*\omega R^2\right). \quad (8)$$

The equation for the *relative* motion, like the one for the CM motion, also possesses a spherical symmetry

$$\left[-\frac{1}{2m^*}\nabla_r^2+\frac{1}{2}m^*\omega_r^2r^2+\frac{1}{2\epsilon r}\right]\varphi(\boldsymbol{r})=E_r\varphi(\boldsymbol{r}),\qquad \omega_r\equiv\frac{1}{2}\omega,\ E'_r\equiv\frac{1}{2}E_r. \quad (9)$$

Its eigenstates are classified in the same way as the oscillator wavefunctions (8)

$$\varphi_{n\ell m}(\boldsymbol{r})=\frac{u_{n\ell}(r)}{\sqrt{m^*r}}Y_{\ell m}(\hat{\boldsymbol{r}}),\qquad n=0,1,2\ldots,\ \ell=0,1,2\ldots. \quad (10)$$

The radial function $u_{n\ell}(r)$ is a solution of the radial Schrödinger equation

$$\left[-\frac{1}{2m^*}\frac{\mathrm{d}^2}{\mathrm{d}r^2}+\frac{1}{2}m^*\omega_r^2r^2+\frac{1}{2}\frac{1}{\epsilon r}+\frac{\ell(\ell+1)}{2m^*}\frac{1}{r^2}\right]u_{n\ell}(r)=\epsilon' u_{n\ell}(r), \quad (11)$$

which can be integrated numerically and in some special cases has an analytical solution [5].

Summarizing this part, the motion of the pair of electrons is described by the independent motions of two quasi-particles, described by the wavefunctions $\xi(\boldsymbol{R})$ and $\varphi(\boldsymbol{r})$ and moving in $\boldsymbol{R}$ and $\boldsymbol{r}$ subspaces, respectively. The two-electron wavefunction is defined by six quantum numbers (N, L, M, n, ℓ, m). The ground state of the two-particle system is constructed from the ground states of the quasi-particles, the excited state is reached whenever any or both of the motions are excited. For simplicity, in the following we restrict our calculations to the quasi-particle wavefunctions with $M = m = 0$. In figure 2 the two-electron wavefunction characterized by different combinations of (N, L, n, ℓ) is shown as a function of (r, R). The number of extrema corresponding to a different degree of excitation of the CM and 'relative' motions can be easily seen. The calculations are made for the confinement frequency $\omega = 0.32$ au. Then the spatial extent of the ground state wavefunction is of the order of 100 Å, which is, in turn, of the order of a typical size of a quantum dot. We used the GaAs effective mass and dielectric constants ($m^* = 0.067$, $\epsilon = 12.4$).

3. DPE probability

In the dipole approximation, the DPE amplitude describing the photon-induced transition between two-electron initial and final states reads

$$T=\langle\Psi_2|\boldsymbol{e}\cdot(\boldsymbol{\nabla}_1+\boldsymbol{\nabla}_2)|\Phi_2\rangle, \quad (12)$$

where $\boldsymbol{e}$ is the photon polarization vector and $(\boldsymbol{\nabla}_1+\boldsymbol{\nabla}_2)$ is a two-particle dipole operator in the velocity form.

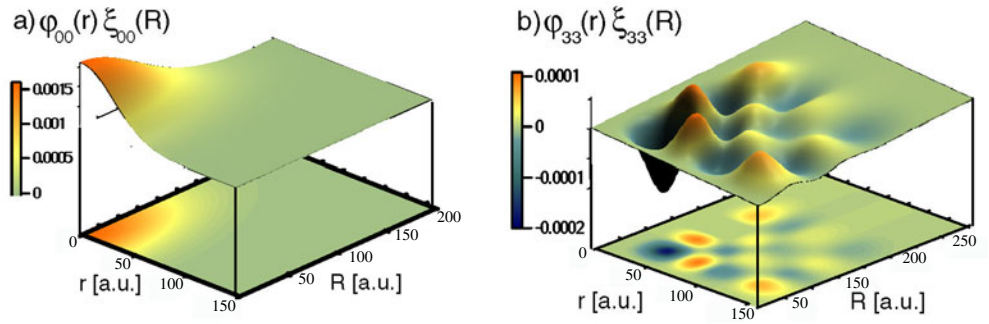

Figure 2. Ground (0, 0, 0, 0) and excited (3, 3, 3, 3) two-particle states of a quantum dot (for its parameters see text) in the CM and relative coordinates.

Although the representation of a quantum dot potential in the form of the infinite harmonian is an idealization, we assume that its low-lying eigenstates reproduce the two-electron states of the real dot qualitatively correctly. Such an approximation significantly simplifies the description of the initial state wavefunction, Φ_2, since for the finite oscillator well the same problem loses separability.

To single out the effect of the initial state correlations, we start from the simplest two-electron final state, constructed as a product of the plane-wave asymptotic detector states, $|\Psi_2\rangle = |\boldsymbol{k}_1\rangle \otimes |\boldsymbol{k}_2\rangle$. The physical justification of this approximation is that after the emission of electrons the quantum dot quickly becomes neutralized by the substrate, so that the final-state three-body interaction between two electrons and an ion is effectively reduced to a two-body interaction between electrons. At the moment we will not even include this kind of interaction. With this approximation, the DPE amplitude factorizes in $(\boldsymbol{r}, \boldsymbol{R})$ space and reduces to a product of the Fourier-transformed wavefunctions for the CM and relative motion

$$T_{k_1k_2} = \langle \boldsymbol{k}_1, \boldsymbol{k}_2 | \boldsymbol{e} \cdot (\boldsymbol{\nabla}_1 + \boldsymbol{\nabla}_2) | \Phi_2 \rangle = \langle \boldsymbol{k}_1 + \boldsymbol{k}_2 | \boldsymbol{e} \cdot \boldsymbol{\nabla} | \xi(\boldsymbol{R}) \rangle \cdot \langle (\boldsymbol{k}_1 - \boldsymbol{k}_2)/2 | \varphi(\boldsymbol{r}) \rangle$$
$$= \boldsymbol{e} \cdot \boldsymbol{Q} \tilde{\xi}(\boldsymbol{Q}) \tilde{\varphi}(\boldsymbol{q}), \tag{13}$$

where we have introduced the CM and 'relative' momenta $\boldsymbol{Q} = \boldsymbol{k}_1 + \boldsymbol{k}_2$ and $\boldsymbol{q} = (\boldsymbol{k}_1 - \boldsymbol{k}_2)/2$, the wavy line denotes the Fourier transform and $\boldsymbol{\nabla}$ is a two-electron momentum operator in $(\boldsymbol{r}, \boldsymbol{R})$ space. In figure 3(a), (b) we plot the square modulus of the transition amplitude as a function of (q, Q). The number of nodes of the wavefunction in the momentum space is the same as in the configuration space and, therefore, the number of maxima in figures 3(a), (b) can be easily identified with the quantum numbers n and N of the corresponding wavefunctions.

Note that the photon transition is contained entirely in the CM part, while the effects of electronic correlation are included only in the 'relative' part of the cross section. Evident experimental use of this factorization is that keeping one of the vectors, $\boldsymbol{Q}$ or $\boldsymbol{q}$, fixed, one can investigate the behaviour of the DPE cross section separately either with respect to correlations, or with respect to the dipole transition.

Let us now mention the properties of the transition amplitude as shown in equation (13).

- The scalar product $\boldsymbol{e} \cdot (\boldsymbol{k}_1 + \boldsymbol{k}_2)$ in equation (13) originates from the approximation used for the final state and serves as a selection rule when $\boldsymbol{e} \cdot (\boldsymbol{k}_1 + \boldsymbol{k}_2) = 0$. The electrons, which are emitted with $\boldsymbol{k}_1 = -\boldsymbol{k}_2$, or whose total momentum is normal to the polarization vector $\boldsymbol{e}$, will not contribute to the cross section.
- The CM wavefunction $\xi(\boldsymbol{R})$ is always symmetric with respect to the particle exchange. Therefore the singlet (triplet) spin part for the two-electron state has to be taken whenever

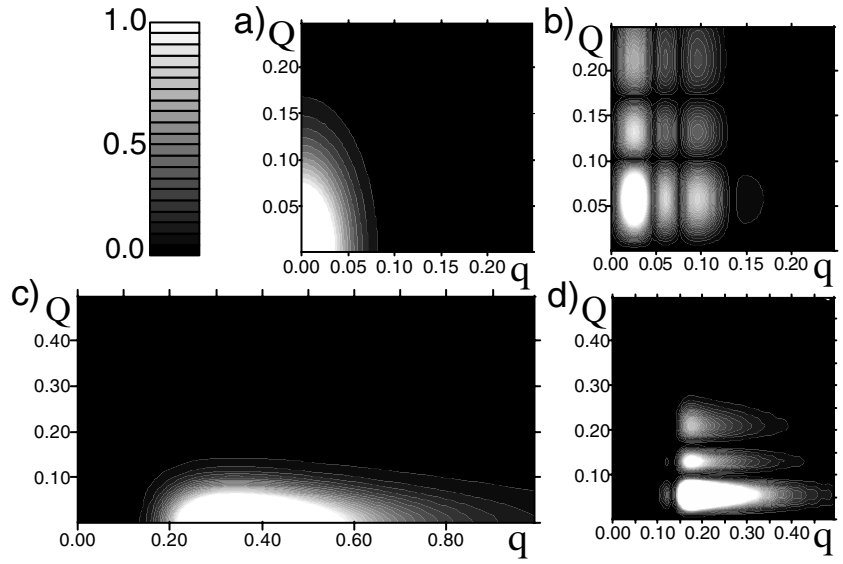

Figure 3. Momentum distribution of a two-particle state in the CM and relative coordinates: (a), (b) ground and excited (2, 2, 2, 2) states; (c), (d) the same as (a) and (b) but multiplied by the density of the final states $\rho(\boldsymbol{k}_1, \boldsymbol{k}_2)$. The black-and-white scale corresponds to a zero-to-one intensity scale.

$\varphi(\boldsymbol{r})$ is even (odd) function. The latter, in turn, is fully specified by the orbital quantum number ℓ in equation (10): even (odd) ℓ values correspond to the singlet (triplet) two-electron states. From this we note another selection rule: two electrons in the triplet state cannot be emitted with $\boldsymbol{k}_1 = \boldsymbol{k}_2$. This is just a consequence of the Pauli principle.

- The third property of the transition amplitude arises from the symmetry constraints on the dipole transition. Namely, the single photoionization dipole selection rules [11, 12] are valid for the matrix element $\langle \boldsymbol{Q}|\boldsymbol{e}\boldsymbol{\nabla}|\xi(\boldsymbol{R})\rangle$. For the given quantum numbers (L, M) of the $\xi_{NLM}(\boldsymbol{R})$, only the components of the final-state CM plane wave with the orbital momenta $L' = L \pm 1$ will be selected. The magnetic quantum numbers M and M' of the initial and final CM states will be connected through the polarization of the photon: $M + \mu = M'$ (the projection of the photon angular momentum $\mu = 0$ for linear and $\mu = \pm 1$ for circular polarization).
- It is only the relative motion that depends on the interaction between electrons. Varying the strength of this interaction leads to a change in shape of the potential well in equation (9) and causes the corresponding change in the localization of $\varphi(\boldsymbol{r})$ and $\tilde{\varphi}(\boldsymbol{q})$: the stronger the Coulomb interaction, the more localized the momentum distribution along the q-coordinate becomes.

The present problem as it is formulated (for the plane-wave final state) can be of use as a checking model for the calculations, employing different forms of initial two-electron states in finite-size systems.

Now we will include the final-state Coulomb interaction between the outgoing electrons. The transition amplitude equation (13) then takes the form

$$T_{\boldsymbol{k}_1\boldsymbol{k}_2} = \langle \boldsymbol{Q}|\boldsymbol{e}\cdot\boldsymbol{\nabla}|\xi(\boldsymbol{R})\rangle \cdot \langle \varphi_{\boldsymbol{q}}^{(-)}(\boldsymbol{r})|\varphi(\boldsymbol{r})\rangle, \tag{14}$$

where $\varphi_{\boldsymbol{q}}^{(-)}(\boldsymbol{r})$ is the Coulomb wave [13]. Its series representation reads [13]

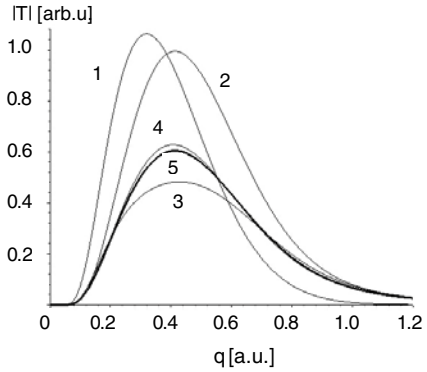

Figure 4. Absolute value of the transition amplitude, $T_{k_1k_2}$, calculated with differing numbers of terms as per the expansion of $\varphi_q^{(-)}(\boldsymbol{r})$, equation (15). The number on each curve corresponds to the number of terms involved, that is, the first curve corresponds to our previous result from figure 3(c) and curve number '5' contains terms in the expansion up to the fifth, which is almost the convergency limit. It is pertinent to note that the series converges quickly because the initial state $\varphi(r)$ is well localized.

$$\varphi_q^{(-)}(\boldsymbol{r}) = N \cdot \mathrm{e}^{\mathrm{i}q\boldsymbol{r}} \cdot {}_1F_1(\mathrm{i}\alpha, 1; -\mathrm{i}(q\boldsymbol{r} + qr))$$
$$= N \cdot \mathrm{e}^{\mathrm{i}q\boldsymbol{r}}\left[1 - \frac{\alpha(q\boldsymbol{r} + qr)}{1!} - \frac{\mathrm{i}\alpha(\mathrm{i}\alpha + 1)}{2!}\frac{(q\boldsymbol{r} + qr)^2}{2!} + \cdots\right], \tag{15}$$

where the Coulomb factor is $N = \exp(-\pi\alpha/2)\Gamma(1 - \mathrm{i}\alpha)$ and the Sommerfeld parameter is $\alpha = 1/q$ [10].

Now, if one accounts only for the first term of this expansion, then, apart from a constant normalization factor, the sixfold differential DPE cross section reads

$$\frac{\mathrm{d}\sigma}{\mathrm{d}E_1\,\mathrm{d}E_2\,\mathrm{d}\Omega_1\,\mathrm{d}\Omega_2} \sim |T_{k_1k_2}|^2\delta(E_R + E_r + \hbar\omega - E_1 - E_2)$$
$$= |\boldsymbol{e} \cdot Q\tilde{\xi}(\boldsymbol{Q})|^2|\tilde{\varphi}(\boldsymbol{q})|^2\rho(q)\delta(E_R + E_r + \hbar\omega - E_1 - E_2), \tag{16}$$

$$\rho(q) \equiv N^2 = \frac{2\pi\alpha}{\exp(2\pi\alpha - 1)}. \tag{17}$$

In this way, the final-state interaction is fully described by the density of final states $\rho(q)$, while the rest of the cross section coincides with the cross section for the non-interacting final-state electrons. The effect of $\rho(q)$ is demonstrated in figure 3(c) ,(d): it monotonically suppresses the emission of the pairs, having small relative momentum, and shifts the positions of the maxima of $|T_{k_1k_2}|^2$ towards higher q values, as can be seen from figures 3(c) ,(d). Qualitatively, this is the only modification, introduced by the inclusion of the repulsive interaction between the final-state electrons. Taking into account the next terms in the series in equation (15) the picture will only change quantitatively as shown in figure 4. Therefore, for the sake of simplicity in the following we will use equation (16).

4. Angular distributions

We present the results in the form of an angular distribution (AD) and an energy sharing distribution (ESD). In the first case, the DPE cross section is plotted as a function of the emission angles (θ_1, ϕ_1) of one electron at fixed emission angles (θ_2, ϕ_2) of the second electron and fixed final state energies E_1 and E_2. In the second case, the DPE cross section is given as a

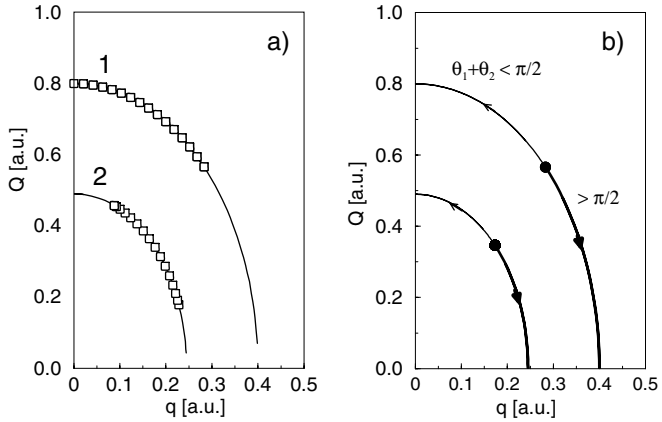

Figure 5. (a): Location of (q, Q) final state momenta contributing to the ADs. Curve 1. $E_{tot} = 0.16$ au, $E_1 = E_2$, full curve, $\theta_2 = 80°$; squares, $\theta_2 = 0°$. Curve 2. $E_{tot} = 0.06$ au, $\theta_2 = 80°$; full curve, $E_1 = E_2$; squares, $E_1 \neq E_2$. (b) Location of (q, Q) final state momenta contributing to the ESDs. Curves 1 and 2 correspond to $E_{tot} = 0.16$ and 0.06 au, respectively. The black circles correspond to $\theta_1 + \theta_2 = 90°$, the left (right) arrow shows the direction when changing the (q, Q)-momenta participating in ESD with a decrease (increase) of $\theta_1 + \theta_2$.

function of the energy difference $(E_1 - E_2)$ for fixed emission directions and fixed total energy $E_{tot} = E_1 + E_2$. We assume that the electron detectors are always placed in the azimuthal plane, i.e. the azimuthal emission angles are $\phi_1 = \phi_2 = 0°$. The polarization vector $\boldsymbol{e}$ of linearly polarized light is chosen along the $(\theta_{ph}, \phi_{ph}) = (0°, 0°)$ direction.

Before coming to the results, it is helpful to visualize the distribution of the final-state momenta that take part in the ADs and ESDs as shown in figures 5(a) and (b), respectively. The relationship between the wavevectors $\boldsymbol{Q}$ and $\boldsymbol{q}$ implies that points with coordinates (q, Q) corresponding to a fixed total final-state energy $E_{tot} = (k_1^2 + k_1^2)/2$ are located on a quarter of an ellipse. The length of the ellipse's axes differs by a factor of 2 due to the difference in the scaled oscillator frequencies, cf equations (6) and (9). Curves 1 and 2 correspond to $E_{tot} = 0.16$ and 0.06 au, respectively. Depending on the experimental setup, the final states with momenta $(\boldsymbol{q}, \boldsymbol{Q})$ arising from the different parts of the ellipse participate in the AD. For example, the solid curves in figure 5(a) depict the pairs (q, Q), corresponding to the grazing emission angle for the 'fixed' electron ($\theta_2 = 80°$), while the first electron is emitted in the range $\theta_1 = 0° \ldots 180°$. The kinetic energies of the two electrons are equal. By decreasing the angle θ_2, the participating arch of the ellipse is made shorter, e.g. at normal emission of the 'fixed' electron ($\theta_2 = 0°$) only the part of the ellipse as shown by the squares in curve 1 is left. Making the kinetic energies of the electrons unequal also cuts off part of the ellipse. In curve 2 the solid curve corresponds to $E_1 = E_2 = 0.03$ au, the square symbols show the range (q, Q) for $E_1 = 0.01$ au, $E_2 = 0.05$ au (for $\theta_2 = 80°$, $\theta_1 = 0° \ldots 180°$). Using these parameters (total kinetic energy, its distribution between electrons, angle of emission) as levers, one can tune through any required region on a (q, Q) map.

To probe the ground state (cf figure 3(c)), we chose $E_{tot} = 0.16$ au (curve 1, figure 5(a)). In figure 6(a), ADs for different $\theta_2 = 85°, 65°, 45°, 0°$ and for $E_1 = E_2 = E_{tot}/2$ are presented. Two maxima on the ADs originate from a single maximum in the ground state wavefunction, damped in the middle by the factor $\boldsymbol{e} \cdot (\boldsymbol{k}_1 + \boldsymbol{k}_2)$, which becomes equal to zero at $\theta_1 = \pi + \theta_2$. Another example is shown in figure 6(b) for the same choice of angles and for $E_{tot} = 0.06$ au (curve 2, figure 5(a)) we plot the DPE ADs from the initial two-particle state (2, 2, 2, 2) (cf figure 3(d)).

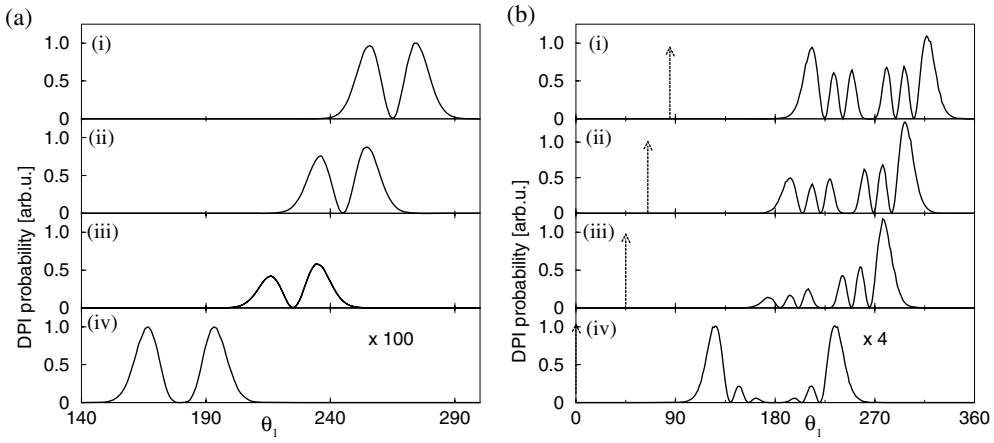

Figure 6. ADs from the ground ((a), $E_{tot} = 0.16$ au) and excited (2, 2, 2, 2) states ((b), $E_{tot} = 0.06$ au) for different θ_2 values. Plots (i)–(iv) correspond to $\theta_2 = 85°, 65°, 45°, 0°$, respectively. The dotted arrow marks the emission direction of the 'fixed' electron, where light is polarized along the $(0°, 0°)$ direction. $E_1 = E_2 = E_{tot}/2$.

5. Energy sharing distributions

An ESD shows how the DPE probability depends on the difference between the individual kinetic energies of two electrons with all the other parameters fixed. First, we note that if the angle between the outgoing electrons is equal to $\pi/2$, only one point on the (q, Q)-map contributes to the cross section (see figure 5(b), black circles). By decreasing or increasing the relative angle, the arches to the left or to the right from this point become 'visible', as shown in figure 5(b). In figure 7(a), this trend is shown in the case of emission from the (2, 2, 2, 2)-state. The angle between the electrons is decreasing ($\theta_1 = -\theta_2 = 85°, 75°, 55°, 45°$), and gradually excludes the maxima of the initial-state density out of the allowed (q, Q)-region. This is shown by the disappearance of the oscillations in the ESDs and also in its magnitude decreasing. In figure 7(b), the importance of choosing the right E_{tot} value is demonstrated for emission from the ground state. Scanning through the single maximum on a (q, Q)-map results in a change in the intensity of the sharing distribution without changing its shape. The minimum in the middle of the ESD is again due to the selection rule; at equal energies the vector $(\boldsymbol{k}_1 + \boldsymbol{k}_2)$ becomes normal to the polarization vector of light.

In conclusion, we have undertaken the analytical and numerical investigation of the mapping of the correlated two-electron state in a parabolic quantum dot by means of DPE. We show that the DPE cross section factorizes into two parts, separately containing the effects due to the dipole transition and due to the electronic correlation. The reconstruction of the two-electron density on the (q, Q) grid, using experimental data, would be straightforwardly traceable in the frames of given approach. Obviously, the present problem can be generalized:

(i) to other forms of electron–electron interaction, dependent only on the distance between the electrons;
(ii) to the description of any nanoparticles that possess oscillator-type potential confinement.

Acknowledgment

The authors are grateful to Manfred Taut for inspiring discussions.

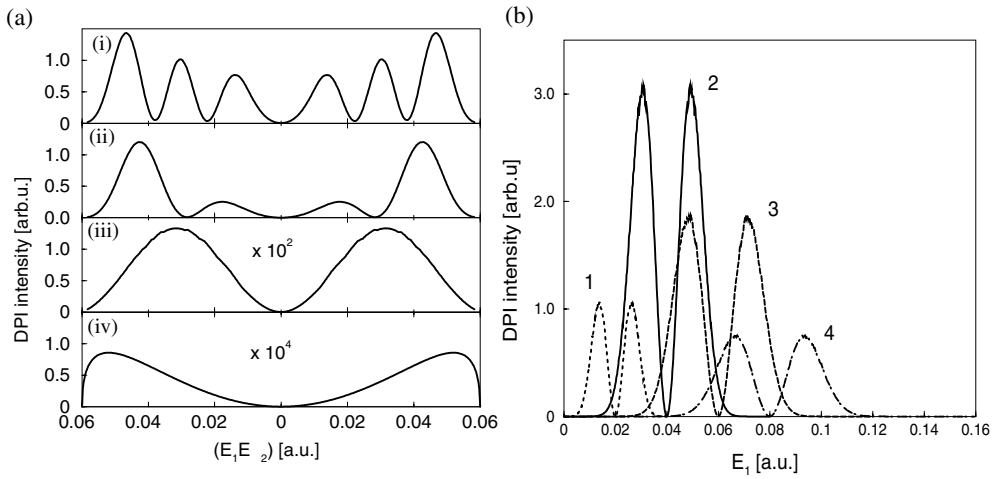

Figure 7. The ESDs from the excited (2, 2, 2, 2) (a) and the ground (b) states. Plots (i)–(iv) in (a) correspond to $\theta_1 = \theta_2 = 85°, 75°, 55°, 45°$. The four curves in (b) correspond to $E_{tot} = 0.04, 0.08, 0.12, 0.16$ au, (note the different abscissae in (a) and (b)).

References

[1] Hüfner S 1995 *Photoelectron Spectroscopy: Principles and Applications* (Berlin: Springer)
[2] Manghi F, Bellini V and Arcangeli C 1997 *Phys. Rev.* B **56** 7149
[3] McCarthy I E and Weigold E 1995 *Electron–Atom Collisions* (Cambridge: Cambridge University Press)
[4] Berakdar J 1998 *Phys. Rev.* B **58** 9808
[5] Taut M 1993 *Phys. Rev.* A **48** 3561
[6] Taut M, Ernst A and Eschrig H 1998 *J. Phys. B: At. Mol. Opt. Phys.* **31** 2689
[7] Jacak L, Hawrylak P and Wojs A 1998 *Quantum Dots* (Berlin: Springer)
[8] Flügge S 1974 *Practical Quantum Mechanics* (Berlin: Springer)
[9] Abramowitz M and Stegun I 1972 *Handbook of Mathematical Functions* (United States: Department of Commerce)
[10] Joachain C J 1979 *Quantum Collision Theory* (Amsterdam: Elsevier)
[11] Amusia M Ya 1990 *Atomic Photoeffect* (New York: Plenum)
[12] Friedrich H 1998 *Theoretical Atomic Physics* (Berlin: Springer)
[13] Landau L D and Lifshitz E M 1958 *Quantum Mechanics: Non-Relativistic Theory* (Oxford: Pergamon)
[14] Gradstein I S and Ryshik I M 1994 *Tables of Integrals, Series and Products* (San Diego, CA: Academic)